



## Synthesis, characterization and application of $\text{Fe}_3\text{O}_4@\text{SiO}_2@\text{PrNH}_2\text{-Cu}$ as a novel and highly efficient magnetic nanocomposite catalyst for the synthesis of $\beta$ -amino ketones via Mannich reaction

Hassan Hassani<sup>a</sup>, Ali Shiri<sup>b</sup> and Maryam Khanali<sup>a</sup>

<sup>a</sup>Department of Chemistry, Payame Noor University, 19395-4697 Tehran, I. R. of Iran

<sup>b</sup>Department of Chemistry, Ferdowsi University of Mashhad, I. R. of Iran

E-mail: hassaniir@yahoo.com

Manuscript received online 31 December 2019, revised and accepted 20 May 2020

An environmentally friendly and efficient procedure has been developed for synthesis of  $\beta$ -amino carbonyls using a copper(II)-propyl amine immobilized on silica-coated  $\text{Fe}_3\text{O}_4$  ( $\text{Fe}_3\text{O}_4@\text{SiO}_2$ ) nanoparticles as a novel and recyclable nanocomposite catalyst. The structure of this new magnetite nanocomposite catalyst was established by thermogravimetric analysis (TGA), FT-infrared spectroscopy (FT-IR), vibrating sample magnetometer (VSM), and X-ray diffraction (XRD) analysis. The catalyst could be recycled four times without much decrease of activity.

Keywords: Magnetite nanocomposite, Mannich reaction, recyclable,  $\beta$ -amino ketones, silica-coated  $\text{Fe}_3\text{O}_4$ .

### Introduction

Heterogeneous solid catalysts have been used as eco-friendly and reusable catalysts in various organic transformations. In recent years, synthesis of new heterogeneous solid catalysts has been the subject of immense interest. Among heterogeneous solid catalysts, magnetic nanoparticles (MNPs) are attractive candidates because of their easy synthesis, high surface area, reusability, low toxicity and cost in chemical processes<sup>1-7</sup>.

In recent decades, MNPs have been used in many fields such as magnetic bio-sensing<sup>8</sup>, cell separation<sup>9,10</sup>, magnetic resonance imaging<sup>11</sup>, optical<sup>12</sup> (towards fluorescent magnetic core shell composites for nitrite optical sensing), chemically modifiable surface<sup>13</sup>, biological<sup>14</sup>, environmental<sup>15</sup> and chemical areas<sup>16</sup>. In addition, MNPs are efficient supported catalysts for organic synthesis<sup>17</sup> because of their large surface to volume ratio and their facile separation from the reaction media by use of a permanent magnetic field.

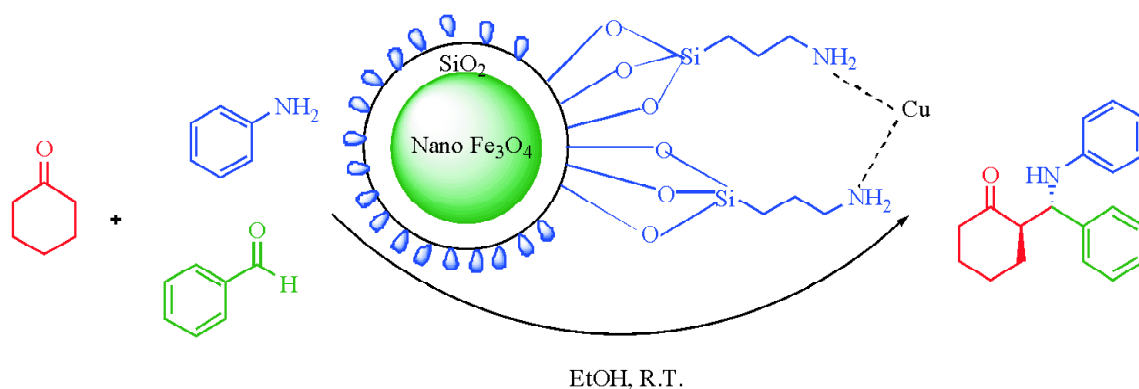
Among magnetic metal oxides,  $\text{Fe}_3\text{O}_4$  particles raised more attention for potential applications in many fields, such as Li-ion batteries<sup>18</sup>, labeling and sorting of cells<sup>19</sup>, absorption and separation<sup>20</sup>, etc. However,  $\text{Fe}_3\text{O}_4$  particles alone

suffer from limitations due to agglomeration, precipitation and oxidation phenomena<sup>21</sup>. In order to overcome such difficulties, an appropriate protection coating is required<sup>22,23</sup>.

Among many materials, silica is considered an important material for the immobilization of NPs due to their chemical stability, slight decrease in the original magnetization<sup>24</sup>, non-toxicity, high-availability, flexibility for surface modification<sup>25-27</sup>. The preparation and the use of  $\text{Fe}_3\text{O}_4@\text{SiO}_2$  as catalysts in organic transformations have been extensively studied in recent years<sup>28,29</sup>. Therefore, present study was devoted to synthesize  $\text{Fe}_3\text{O}_4@\text{SiO}_2$  nanocomposite via tetraethyl orthosilicate and then functionalization by 3-aminopropyltrimethoxysilane (APTMS) to obtain  $\text{Fe}_3\text{O}_4@\text{SiO}_2@\text{PrNH}_2$ .

$\text{Fe}_3\text{O}_4@\text{SiO}_2$  amino-functionalized nanoparticles are important for various applications in drug targeting, protein purification and water treatment<sup>30</sup>.

Mannich reaction is one of the most important carbon-carbon bond forming reactions in organic chemistry for the preparation of secondary and tertiary amines<sup>31,32</sup>. The products of Mannich reaction are mainly  $\beta$ -amino carbonyl compounds, which are important synthetic intermediates for various amino alcohols, peptides and lactams, amino acids phar-



Scheme 1

maceuticals and natural products<sup>33,31</sup>.  $\beta$ -Amino ketones are generally obtained by the condensation of a carbonyl compound with an aldehyde and an amine using organic or mineral acids like proline<sup>34</sup>, *p*-dodecyl benzene sulphonic acid<sup>35</sup>,  $\text{CeCl}_3 \cdot 7\text{H}_2\text{O}$ <sup>36</sup>, nano- $\text{TiO}_2$ <sup>37</sup>, phosphorodiamidic acid<sup>38</sup>,  $\text{ZnCl}_2/\text{SiO}_2$ <sup>39</sup>. Although some of these methods are advantageous, drawbacks such as low yields, long reaction times, harsh reaction conditions, toxicity and moisture sensitivity of the catalysts, tedious workup of the reaction mixture and recovery of the catalyst create much problem. This has demanded the development of efficient, high yielding, inexpensive and environmentally benign methods for the Mannich reaction. In continuation of our previous works on the design, synthesis and use of magnetic nano-catalysts, we report herein the preparation of  $\text{Fe}_3\text{O}_4@\text{SiO}_2@\text{prNH}_2\text{-Cu(II)}$  as illustrated in Scheme 1 and its use as a magnetic nano catalyst for efficient synthesis of  $\beta$ -amino carbonyl compounds by condensation of cyclohexanone, aromatic aldehydes and aromatic amines.

## Experimental

### Chemicals:

All solvents and reagents were purchased from Sigma-Aldrich (USA) and Merck (Germany) Chemical Companies. The purity of the products and the progress of the reactions were determined by TLC on silica-gel Polygram SILG/UV254 plates. Melting points were measured on an Electro thermal 9100 apparatus. IR spectra were obtained on a Perkin-Elmer 781 spectrometer as KBr pellets and reported in  $\text{cm}^{-1}$ .  $^1\text{H}$  NMR and  $^{13}\text{C}$  NMR spectra were measured on a Bruker DPX-

250 Advance instrument at 250 MHz and 62.9 MHz, respectively, in  $\text{CDCl}_3$  with the chemical shift reported in ppm relative to TMS as an internal standard. Powder X-ray diffraction (XRD) was performed on a Bruker D8-advance X-ray diffractometer with  $\text{Cu K}\alpha$  ( $1 \frac{1}{4}$  0.154 nm) radiation. The thermogravimetric analysis (TGA) curves were recorded under air atmosphere using a TGA/DTA Shimadzu-50 with a platinum pan. The samples were heated in air from 25 to  $800^\circ\text{C}$  with a heating rate of  $10^\circ\text{C}/\text{min}$ . The magnetic properties were determined using a vibrating sample magnetometer (VSM) lakeshore 7200 at 300 K VSM lakeshore.

### Catalyst preparation:

#### Preparation of the $\text{Fe}_3\text{O}_4$ nanoparticles:

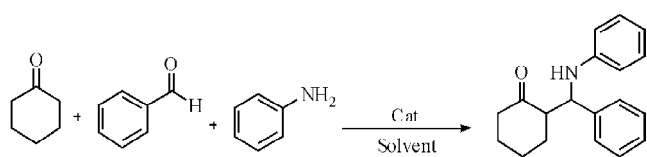
$\text{Fe}_3\text{O}_4$  nanoparticles were synthesized by the co-precipitation of  $\text{Fe}^{3+}$  and  $\text{Fe}^{2+}$  ions<sup>40</sup>.

Typically, sodium hydroxide (15 g) was dissolved into deionized water (25 mL). Thereafter, a mixture of  $\text{FeCl}_2 \cdot 4\text{H}_2\text{O}$  (2 g),  $\text{FeCl}_3 \cdot 6\text{H}_2\text{O}$  (5.2 g), deionized water (25 mL) and of 12 M HCl (0.85 mL) was added drop wise under the condition of vigorously stirring to make a black solid product. The resulting material was left to be stirred for 4 h at  $80^\circ\text{C}$  in an oil bath under  $\text{N}_2$  atmosphere. The obtained  $\text{Fe}_3\text{O}_4$  magnetic nanoparticles were separated using a magnet and washed three times with water and then dried in an oven at  $80^\circ\text{C}$  for 10 h.

#### Preparation of the $\text{Fe}_3\text{O}_4@\text{SiO}_2$ :

$\text{Fe}_3\text{O}_4$  (0.5 g) was dispersed in a mixture of ethanol (100 mL) and deionized water (20 mL) and predisposed by ultrasonic device for 10 min. Then,  $\text{NH}_3$  (27%, 2.5 mL) was added

**Table 1.** Optimization of the reaction conditions



Entry	Solvent	Catalyst (g)	Time (min)	Yield (%)
1	$\text{CH}_2\text{Cl}_2$	0.03	80	70
2	$\text{CHCl}_3$	0.03	85	72
3	$\text{CH}_3\text{CN}$	0.03	60	83
4	$\text{H}_2\text{O}$	0.03	60	80
5	Solvent-free	0.03	40	85
6	EtOH	0.03	30	95
7	EtOH	0.04	30	95
8	EtOH	0.05	10	96
9	EtOH	0.06	15	92
10	EtOH	0.02	50	90

<sup>a</sup>Reaction conditions: solvent (1 mL), room temperature, benzaldehyde (1 mmol), aniline (1 mmol), cyclohexanone (1.1 mmol).

followed by the drop wise addition of tetraethoxysilane (TEOS) (1.5 mL). After vigorous stirring for 6 h at room temperature the final product  $\text{Fe}_3\text{O}_4@\text{SiO}_2$  was separated using an external magnet and was washed three times with deionized water and ethanol, and then dried at  $80^\circ\text{C}$  for 10 h<sup>41</sup>.

#### Preparation of $\text{Fe}_3\text{O}_4@\text{SiO}_2$ bonded propylamine:

The  $\text{Fe}_3\text{O}_4@\text{SiO}_2$  was functionalized by amine group according to a method reported in the literature<sup>42</sup>.  $\text{Fe}_3\text{O}_4@\text{SiO}_2$  MNPs (1 g) dispersed in of dry toluene (100 mL) was subjected to vigorous stirring and to the mixture 3-(trimethoxysilyl)-propylamine (2.5 mL) was added. Afterwards, NaH (0.008 g) was added and the resulting suspension was refluxed for 48 h. After refluxing, the mixture was cooled to room temperature, and then the final product was collected by an external magnet.  $\text{Fe}_3\text{O}_4@\text{SiO}_2@\text{PrNH}_2$  MNPs was washed three times with dry toluene and ethanol (each), and then dried under vacuum at  $80^\circ\text{C}$  for 4 h.

#### Preparation of $\text{Fe}_3\text{O}_4@\text{SiO}_2@\text{PrNH}_2$ magnetic nanoparticles (MNPs) functionalized with copper(II):

$\text{Fe}_3\text{O}_4@\text{SiO}_2@\text{PrNH}_2$  (1 g) was added to a solution of  $\text{Cu}(\text{OAc})_2$  (3 g) in ethanol (2 mL) and the reaction mixture

was heated at  $60^\circ\text{C}$  for 4 h. The resulting  $\text{Fe}_3\text{O}_4@\text{SiO}_2@\text{PrNH}_2\text{-Cu}$  nanoparticles were collected using an external magnetic field, and finally dried at  $60^\circ\text{C}$  for 4 h.

#### Catalytic activity:

#### General procedure for the preparation of $\beta$ -amino ketones:

To a mixture of the aromatic aldehyde (2 mmol), aromatic amines (2 mmol) and cyclohexanone (2.2 mmol) in ethanol (2 mL) was added  $\text{Fe}_3\text{O}_4@\text{SiO}_2@\text{PrNH}_2\text{-Cu}$  MNPs (0.1 g) and the reaction mixture was stirred at room temperature for an appropriate time (Table 2). After completion of the reaction, the mixture was diluted with hot ethanol (15 mL) and the catalyst was separated with an external magnet. The sole product of Mannich reaction was crystallized after reducing the volume of ethanol and cooling.

## Results and discussion

The synthetic route to  $\text{Fe}_3\text{O}_4@\text{PrNH}_2\text{-Cu}$  MNPs is shown in Scheme 2. First,  $\text{Fe}_3\text{O}_4$  MNPs were prepared by the reaction of  $\text{FeCl}_2\cdot 4\text{H}_2\text{O}$ ,  $\text{FeCl}_3\cdot 6\text{H}_2\text{O}$  with sodium hydroxide in deionized water. For the preparation of core-shell catalyst, to a mixture of  $\text{Fe}_3\text{O}_4$  and tetraethoxysilane (TEOS) was added  $\text{NH}_3$ , which was stirred at room temperature to produce the  $\text{Fe}_3\text{O}_4@\text{SiO}_2$  MNPs. Then, the  $\text{Fe}_3\text{O}_4@\text{SiO}_2$  core-shell was reacted with 3-(trimethoxysilyl)-propylamine in dry toluene for 48 h in the presence of NaH to give  $\text{Fe}_3\text{O}_4@\text{SiO}_2@\text{PrNH}_2$ . Finally,  $\text{Cu}(\text{OAc})_2$  was added to obtain the  $\text{Fe}_3\text{O}_4@\text{SiO}_2@\text{PrNH}_2\text{-Cu}$  nanocatalyst.

#### Characterization of the $\text{Fe}_3\text{O}_4@\text{SiO}_2@\text{PrNH}_2$ and $\text{Fe}_3\text{O}_4@\text{SiO}_2@\text{PrNH}_2\text{-Cu}$ MNPs:

The structure of synthesized catalyst was established through FT-IR, TGA, VSM, and XRD studies.

#### FT-IR studies:

Fig. 1 shows the FT-IR spectra of  $\text{Fe}_3\text{O}_4@\text{SiO}_2$  and  $\text{Fe}_3\text{O}_4@\text{SiO}_2@\text{PrNH}_2$ . As shown in Fig. 1a, the characteristic peak near  $630\text{--}650\text{ cm}^{-1}$  can be attributed to the Fe-O bond. The peaks at  $1105\text{--}1120\text{ cm}^{-1}$  and  $980\text{--}993\text{ cm}^{-1}$  are corresponding to the Si-O. In Fig. 1b, the broad characteristic band located at  $3420\text{ cm}^{-1}$  can be attributed to the symmetric vibration of  $\text{-NH}_2$  groups.

**Table 2.** Synthesis of  $\beta$ -aminocarbonyl compounds derivatives  $\text{Fe}_3\text{O}_4@\text{SiO}_2@\text{PrNH}_2\text{-Cu}$ 

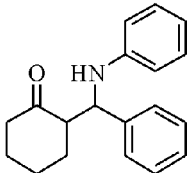
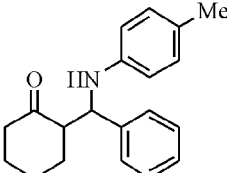
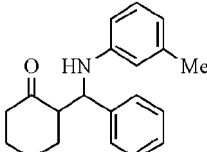
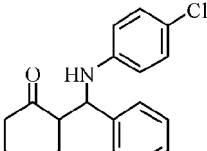
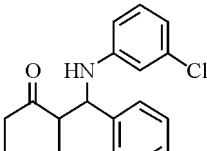
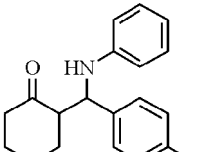
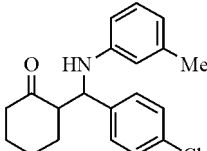
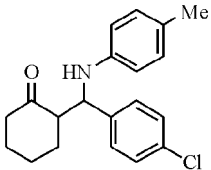
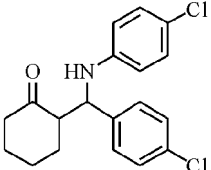
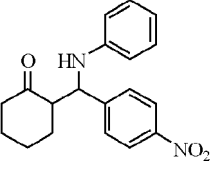
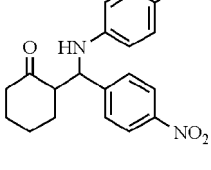
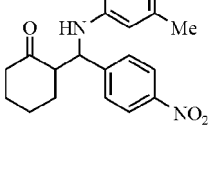
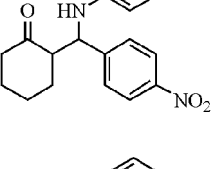
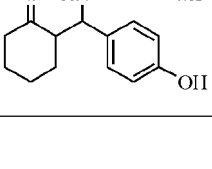
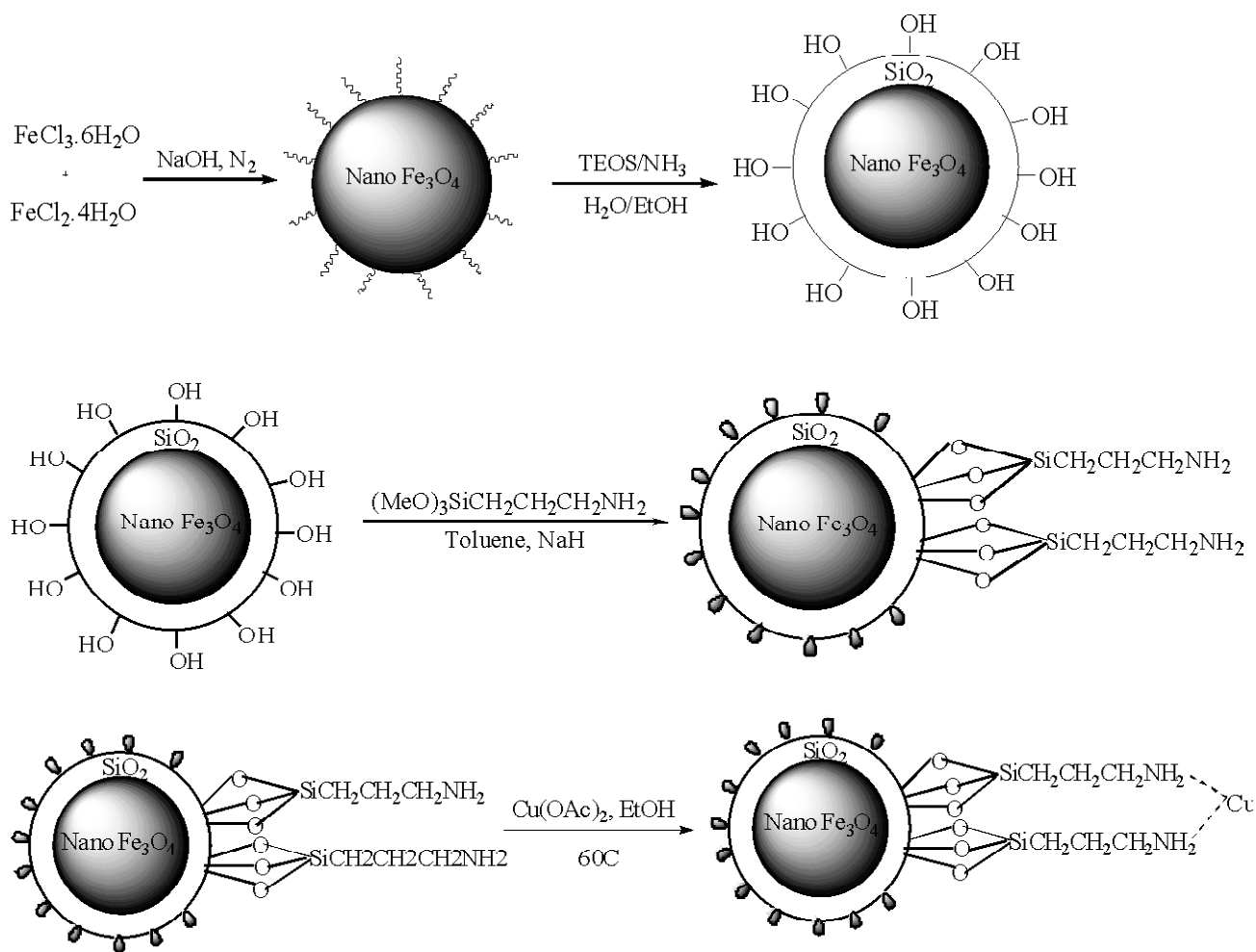
Entry	R <sub>1</sub>	R <sub>2</sub>	Product	Time (min)	Yield (%)	m.p. (°C) [lit. value]
1	H	H		10	96	127–129 [128–129] (Ref. 45)
2	H	4-Me		25	90	119–121 [116–118] (Ref. 46)
3	H	3-Me		10	88	124–126 [123–124] (Ref. 47)
4	H	4-Cl		10	93	134–136 [137–138] (Ref. 45)
5	H	3-Cl		15	91	130–132 [122–123] (Ref. 45)
6	4-Cl	H		25	91	131–133 [135–136] (Ref. 48)
7	4-Cl	3-Me		20	90	126–128 [127–128] (Ref. 49)

Table-2 (contd.)

8	4-Cl	4-Me		25	88	122–124 [119–121] (Ref. 50)
9	4-Cl	4-Cl		25	89	134–136 [98–99] (Ref. 51)
10	4-NO <sub>2</sub>	H		20	85	121–123 [123–125] (Ref. 52)
11	4-NO <sub>2</sub>	4-Cl		30	77	165–167 [169–171] (Ref. 47)
12	4-NO <sub>2</sub>	3-Me		20	80	159–161 [161–162] (Ref. 49)
13	4-NO <sub>2</sub>	4-Me		35	75	139–141 [137–138] (Ref. 51)
14	4-OH	3-Me		12	88	185–187 [181–183] (Ref. 53)



**Scheme 2.** Preparation of the Fe<sub>3</sub>O<sub>4</sub>@SiO<sub>2</sub>@PrNH<sub>2</sub>-Cu MNPs.

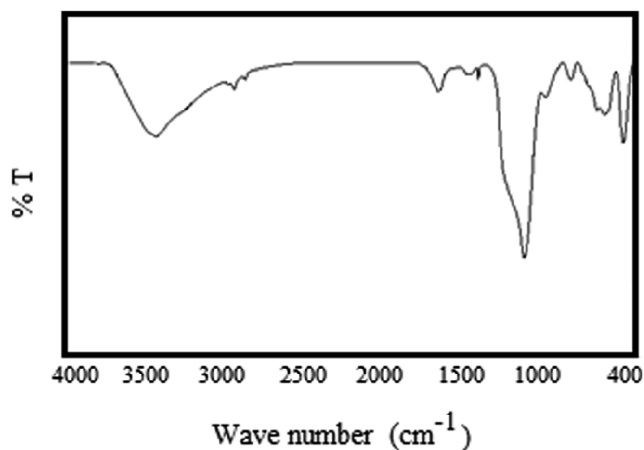
*XRD studies:*

Fig. 2 presents the X-ray diffraction (XRD) patterns of (a) Fe<sub>3</sub>O<sub>4</sub>, (b) Fe<sub>3</sub>O<sub>4</sub>@SiO<sub>2</sub> and (c) Fe<sub>3</sub>O<sub>4</sub>@SiO<sub>2</sub>@PrNH<sub>2</sub>. As it is observed in Fig. 2a, the main characteristic peaks of Fe<sub>3</sub>O<sub>4</sub> are located at 2θ = 30.2 (220), 35.3 (311), 43.2 (400), 53.5 (422), 57 (511), 62.5 (440). These peaks are in agreement with the standard pattern of 19-629 (JCPDS) for the highly crystalline spinel cubic structure of Fe<sub>3</sub>O<sub>4</sub><sup>43</sup>. In the case of Fe<sub>3</sub>O<sub>4</sub>@SiO<sub>2</sub> (Fig. 2b), all of these peaks are also found which showed that the crystalline structure of Fe<sub>3</sub>O<sub>4</sub> remained on its surface. The broad peak from 2θ = 15–25 is attributed to the amorphous SiO<sub>2</sub> layer. Also, the crystal size of Fe<sub>3</sub>O<sub>4</sub>@SiO<sub>2</sub>@PrNH<sub>2</sub> was determined from the X-ray patterns using the Debye-Scherrer formula given as  $D = K\lambda/\beta$

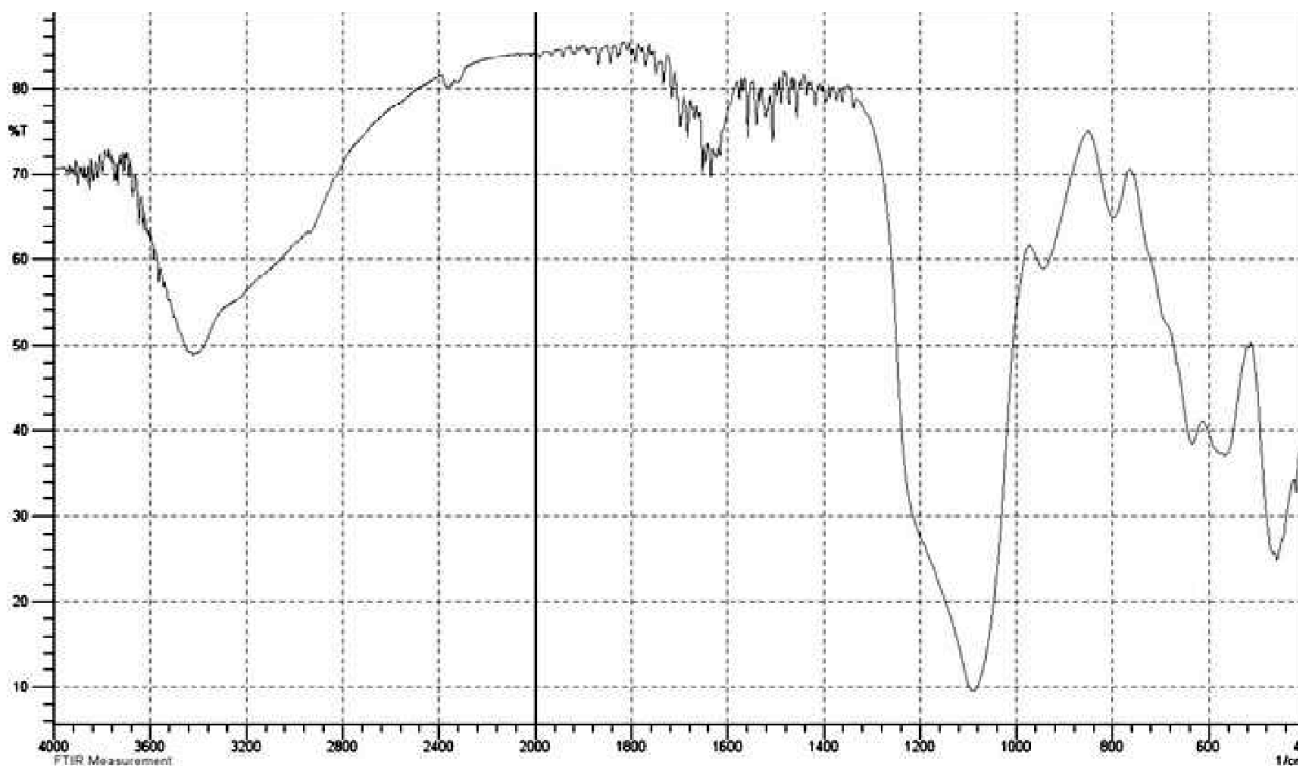
$\cos\theta$ , where  $D$  is the average crystal size,  $K$  is the Debye-Scherrer constant (0.9),  $\lambda$  the X-ray wavelength used (1.54 Å),  $\beta$  the angular line width at a half maximum intensity and  $\theta$  the Bragg's angle. The average crystal size of the Fe<sub>3</sub>O<sub>4</sub>@SiO<sub>2</sub>@PrNH<sub>2</sub> was calculated to be around 12.5–15 nm.

*TGA studies:*

Thermogravimetric analysis (TGA) was usually used to determine the content of functional groups and magnetic content of the particles. Fig. 3 presents the TGA of the Fe<sub>3</sub>O<sub>4</sub>@SiO<sub>2</sub>@PrNH<sub>2</sub> prepared. It can be seen 5% weight loss was observed at around 180°C to 600°C and this indicates release of water and decomposition of aminopropyl groups on the Fe<sub>3</sub>O<sub>4</sub>@SiO<sub>2</sub>@PrNH<sub>2</sub> nanoparticles.



(a)



(b)

**Fig. 1.** (a) The FT-IR spectrum of the  $\text{Fe}_3\text{O}_4@\text{SiO}_2$  and (b) the FT-IR spectrum of the  $\text{Fe}_3\text{O}_4@\text{SiO}_2@\text{PrNH}_2$  MNPs.

#### VSM studies:

VSM analysis was carried out to assess the magnetic properties of  $\text{Fe}_3\text{O}_4@\text{SiO}_2@\text{PrNH}_2$ . Fig. 4 illustrates magnetization versus magnetic field for the  $\text{Fe}_3\text{O}_4@\text{SiO}_2@\text{PrNH}_2$  nanoparticles. As it obvious in Fig. 4, the saturation mag-

netization of MNPs was 32.12 emu/g.

#### Determination of Cu(II) in $\text{Fe}_3\text{O}_4@\text{SiO}_2@\text{PrNH}_2\text{-Cu}$ MNPs:

The  $\text{Fe}_3\text{O}_4@\text{SiO}_2@\text{PrNH}_2\text{-Cu}$  MNPs was dispersed to the solution of AcOH in ethanol. Then,  $\text{K}_4\text{Fe}(\text{CN})_6$  was added

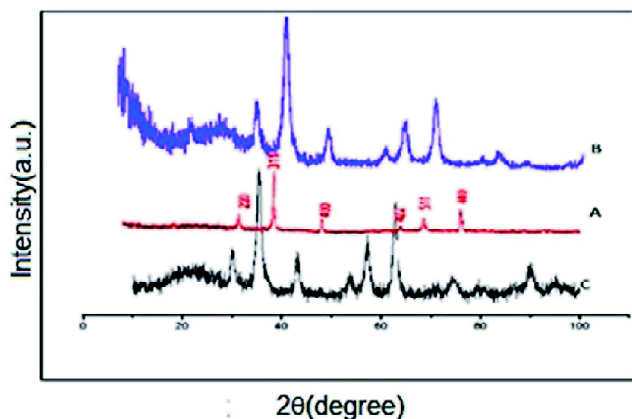


Fig. 2. XRD pattern of (a) Fe<sub>3</sub>O<sub>4</sub> MNPs, (b) Fe<sub>3</sub>O<sub>4</sub>@SiO<sub>2</sub> MNPs and (c) Fe<sub>3</sub>O<sub>4</sub>@SiO<sub>2</sub>@PrNH<sub>2</sub> MNPs.

*Catalytic studies:*

After characterization of catalyst, in order to investigate the catalytic activity of the Fe<sub>3</sub>O<sub>4</sub>@SiO<sub>2</sub>@PrNH<sub>2</sub>-Cu, the catalyst was used in the synthesis of β-amino carbonyl compounds via one-pot reaction of substituted anilines and benzaldehydes with cyclohexanone. In order to achieve the best experimental conditions, initially we chose the reaction of aniline (1 mmol, 0.09 g) and benzaldehyde (1 mmol, 0.106 g) with cyclohexanone (1.1 mmol, 0.1 g) as a reaction model (Scheme 1). Initially, the model reaction was carried out in several solvents such as EtOH, H<sub>2</sub>O, CH<sub>3</sub>CN, CHCl<sub>3</sub>, and CH<sub>2</sub>Cl<sub>2</sub> and under solvent-free conditions at room temperature. The results are summarized in Table 1. As shown in

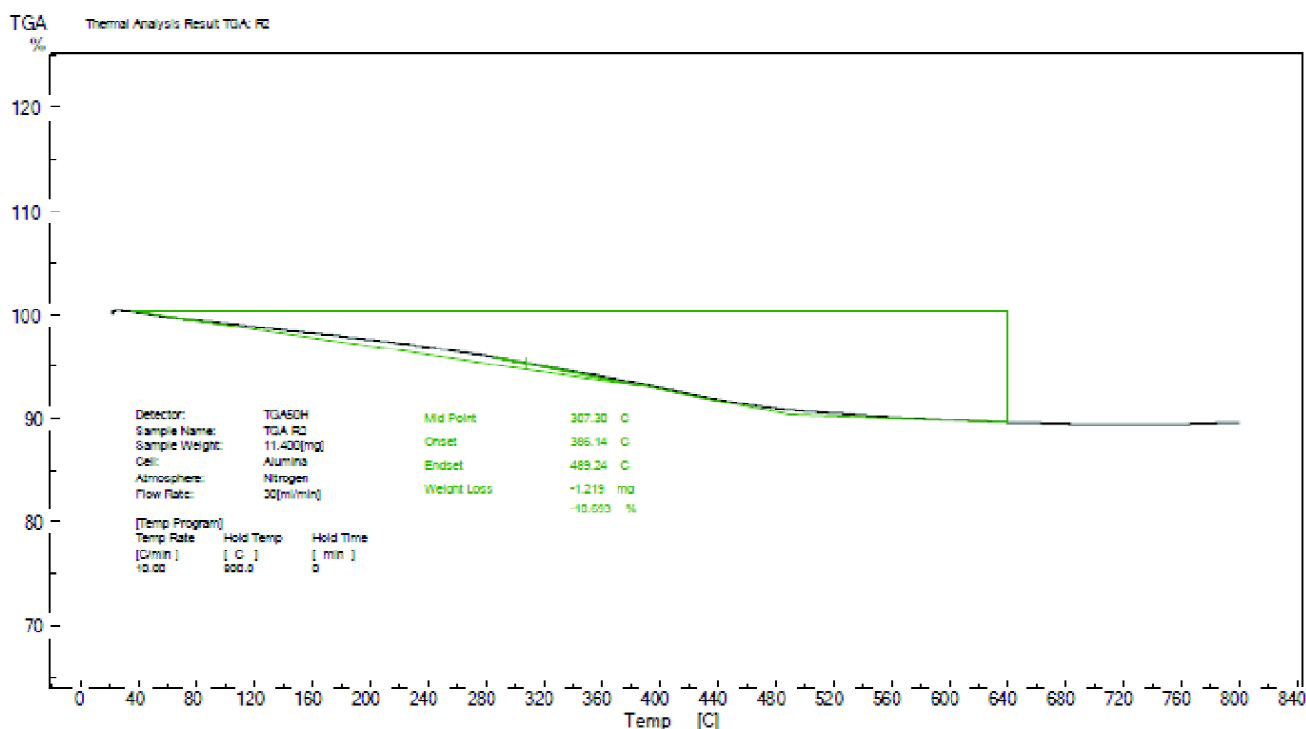


Fig. 3. TGA analysis of Fe<sub>3</sub>O<sub>4</sub>@SiO<sub>2</sub>@PrNH<sub>2</sub> MNPs.

drop by drop to the mixture. The hexacyanoferrate(II) ion reacts with the copper ion to produce the deep rose copper(II) hexacyanoferrate(II) precipitate and the color of the mixture changed to dark red.

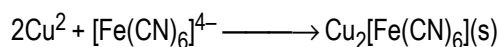


Table 1, in aprotic solvents such as CH<sub>2</sub>Cl<sub>2</sub>, CHCl<sub>3</sub> and CH<sub>3</sub>CN, desired product was isolated in 70, 72 and 83% yield respectively, along with unconsumed imine as side-product. When the reaction was performed in EtOH, the desired product was isolated in good yield in short time with high selectivity. When the reaction was performed in solvent-free



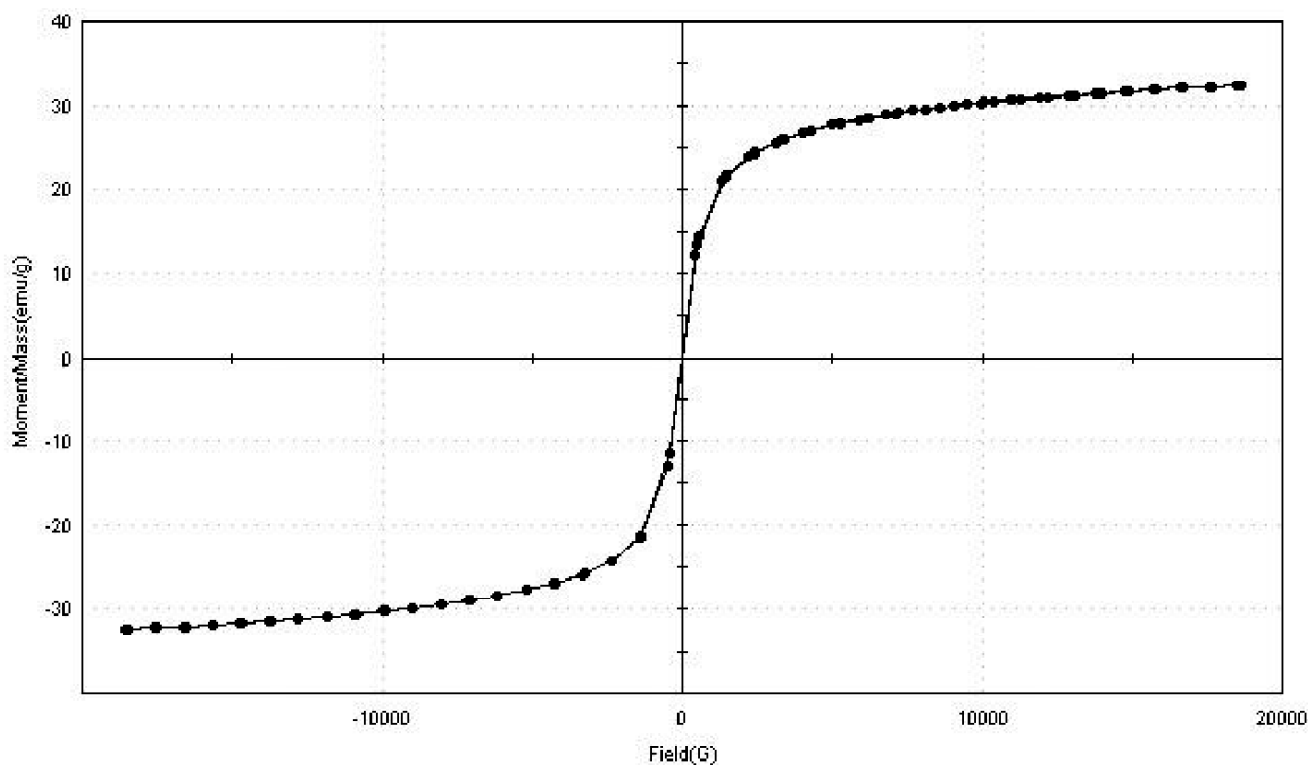


Fig. 4. The VSM pattern of the  $\text{Fe}_3\text{O}_4@\text{SiO}_2@\text{PrNH}_2$  MNPs.

condition, the reaction did not progress efficiently, and the desired product was obtained in moderate yield. Therefore, EtOH was selected as the solvent in further investigations.

In the next step, this reaction was tested in the presence of different ratios of the  $\text{Fe}_3\text{O}_4@\text{SiO}_2@\text{PrNH}_2\text{-Cu}$  MNPs (Table 1, entries 6–10). In absence of the nanocatalyst, no products were produced even after higher reaction time. As the results show, the best outcome was obtained with the use of 0.05 g in ethanol at room temperature. No improvement in the yield was found by use of higher amount of the catalyst while lower amount of the catalyst decreased the yield.

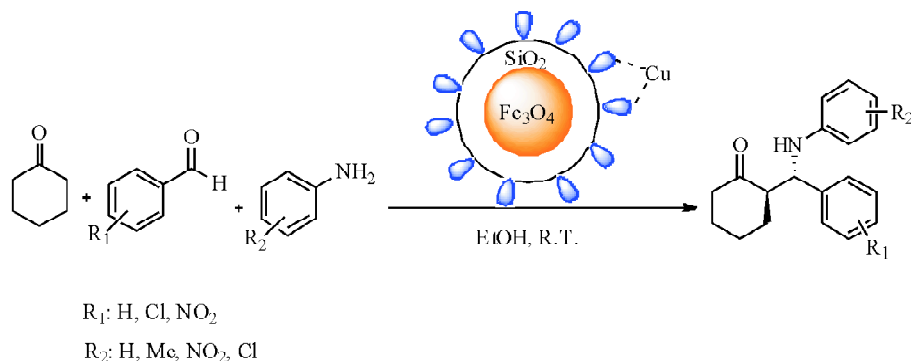
To display the general applicability of this protocol, the reactions of different aromatic aldehydes, anilines and cyclohexanone were carried out at room temperature in ethanol as the solvent. The results are summarized in Table 2. It was observed in all cases the desired product was obtained in good to high yields with good distereoselectivity. It was observed that under the optimized reaction conditions the

substrates with electron-donating groups were more reactive than those carrying electron-withdrawing groups (Scheme 3).

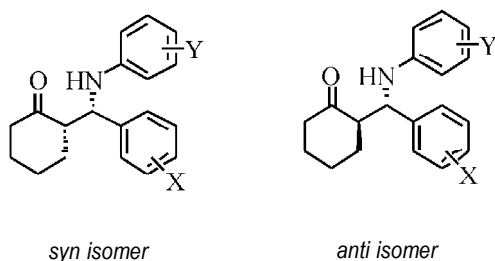
Configurations of the *anti* and *syn* isomers were determined by the coupling constants ( $J$ ) of the vicinal protons adjacent to C=O and NH in their  $^1\text{H}$  NMR spectra and by comparing our data with that of known compounds reported in the literature<sup>44</sup>. In general, the coupling constant of the *anti* isomer is higher than that of the *syn* isomer.

*Physical and spectroscopic data of selected compounds:*

*2-(Phenyl(phenylamino)methyl)cyclohexanone* (Table 2, entry 1): Yield: 96%, white solid, *syn/anti*: 1/99, FT-IR:  $\nu_{\text{max}}$  (KBr): 3329 (NH stretch), 1701 (C=O stretch)  $\text{cm}^{-1}$ ;  $^1\text{H}$  NMR (250 MHz,  $\text{CDCl}_3$ ):  $\delta$  1.55–1.92 (m, 6H,  $\text{CH}_2$ ), 2.25–2.44 (m, 2H,  $\text{CH}_2$ ), 2.7–2.8 (m, 1H, CH), 4.67 (d,  $J$  7.0 Hz, 0.99H, CH), 4.81 (d,  $J$  4.38 Hz, 0.01H, CH), 7.07–7.21 (m, 5H, CH Ar), 7.23–7.55 (m, 5H, CH Ar) ppm;  $^{13}\text{C}$  NMR ( $\text{CDCl}_3$ ):  $\delta$  23.67, 27.92, 31.31, 41.8, 57.5 (C), 57.8, 113.6, 117.5, 127.2, 128.5, 129.1, 130.4, 141.8, 141.3, 212.8 ppm. Anal. Calcd.



Scheme 3



for C<sub>19</sub>H<sub>21</sub>NO (279.36): C, 81.68; H, 7.58; N, 5.01. Found: C, 81.49; H, 7.69; N, 4.95. MS (EI) *m/z* 279 (M<sup>+</sup>).

2-(Phenyl-*p*-tolylamino-methyl)cyclohexanone (Table 2, entry 2): Yield: 90%, white solid, *syn/anti*: 7/93, FT-IR:  $\nu_{\max}$  (KBr): 3332 (NH stretch), 1708 (C=O stretch) cm<sup>-1</sup>; <sup>1</sup>H NMR (250 MHz, CDCl<sub>3</sub>):  $\delta$  1.62–1.90 (m, 6H, 3CH<sub>2</sub>), 2.23–2.41 (m, 2H, CH<sub>2</sub>), 2.45 (s, 3H, CH<sub>3</sub>), 2.7–2.8 (m, 1H, CH), 4.50 (br, 1H, NH), 4.63 (d, *J* 3.5 Hz, 0.93H, CH), 4.79 (d, *J* 3.5 Hz, 0.07H, CH), 6.40–6.53 (m, 2H, 12, CH Ar), 6.82–6.97 (m, 2H, 13, CH Ar), 7.18–7.45 (m, 5H, CH Ar) ppm. Anal. Calcd. for C<sub>20</sub>H<sub>23</sub>NO: C, 81.87; H, 7.90; N, 4.77. Found: C, 81.33; H, 8.13; N, 4.61. MS (EI) *m/z* 293 (M<sup>+</sup>).

2-(Phenyl-*m*-tolylamino-methyl)cyclohexanone (Table 2, entry 3): Yield: 88%, cream solid; *syn/anti*: 0/100, FTIR:  $\nu_{\max}$  (KBr): 3382 (NH stretch), 1693 (C=O stretch) cm<sup>-1</sup>; <sup>1</sup>H NMR (300 MHz, CDCl<sub>3</sub>):  $\delta$  1.61–2.08 (m, 6H, 3CH<sub>2</sub>), 2.21 (s, 3H, CH<sub>3</sub>), 2.23–2.48 (m, 2H, CH<sub>2</sub>), 2.79–2.86 (m, 1H, CH), 4.84 (d, *J* 6.0 Hz, 1H, CH), 6.36–6.52 (m, 3H, CH Ar), 6.97–7.02 (m, 1H, CH Ar), 7.21–7.40 (m, 5H, CH Ar) ppm. Anal. Calcd. for C<sub>20</sub>H<sub>23</sub>NO: C, 81.87; H, 7.90; N, 4.77. Found: C, 80.98; H, 8.19; N, 4.52.

2-((4-Chlorophenylamino) (phenyl)methyl)cyclohexanone (Table 2, entry 4): Yield: 93%, white solid, *syn/anti*: 0/100, FT-IR:  $\nu_{\max}$  (KBr): 3379 (NH stretch), 1705 (C=O stretch) cm<sup>-1</sup>; <sup>1</sup>H NMR (300 MHz, CDCl<sub>3</sub>): 1.71–1.96 (m, 6H, 3CH<sub>2</sub>), 2.36–2.40 (m, 1H, CH<sub>2</sub>), 2.54–2.58 (m, 1H, CH<sub>2</sub>), 2.84–2.88 (m, 1H, CH), 3.86 (br, 1H, NH), 4.23 (m, 1H, CH), 6.93 (d, *J* 8.4 Hz, 2H, 13, CH Ar) ppm. Anal. Calcd. for C<sub>19</sub>H<sub>20</sub>NOCl: C, 72.72; H, 6.42; N, 4.46. Found: C, 73.98; H, 6.74; N, 4.01.

2-((3-Chlorophenylamino)(phenyl) methyl)cyclohexanone (Table 2, entry 5): Yield: 91%, cream solid, *syn/anti*: 0/100, FT-IR:  $\nu_{\max}$  (KBr): 3340 (NH stretch), 1701 (C=O stretch) cm<sup>-1</sup>; <sup>1</sup>H NMR (300 MHz, CDCl<sub>3</sub>): 1.69–2.01 (m, 6H, 3CH<sub>2</sub>), 2.31–2.47 (m, 2H, CH<sub>2</sub>), 2.76–2.82 (m, 1H, CH<sub>2</sub>), 4.58 (d, *J* 6.6 Hz, 1H, CH), 4.92 (br, NH), 6.41–6.45 (m, 1H, CH Ar), 6.53–6.56 (m, 1H, CHAr), 6.53–6.56 (m, 1H, CH Ar), 6.59–6.63 (m, 1H, CH Ar), 6.96–7.01 (m, 1H, CH Ar), 7.24–7.40 (m, 4H, CH Ar) ppm. Anal. Calcd. for C<sub>19</sub>H<sub>20</sub>NOCl: C, 72.72; H, 6.42; N, 4.46. Found: C, 72.65; H, 6.34; N, 4.65.

2-[[4-Chloro-phenyl]-*m*-tolylamino-methyl]cyclohexanone (Table 2, entry 7): Yield: 90%, beige solid, *syn/anti*: 0/100, FT-IR:  $\nu_{\max}$  (KBr): 3348 (NH stretch), 1701 (C=O stretch) cm<sup>-1</sup>; <sup>1</sup>H NMR (CDCl<sub>3</sub>):  $\delta$  1.71–1.92 (m, 6H, 3CH<sub>2</sub>), 2.19 (s, 3H, CH<sub>3</sub>), 2.31–2.54 (m, 2H, CH), 2.87–2.89 (m, 1H, CH), 4.59 (d, *J* 6.25 Hz, 1H, CH), 6.28–6.36 (m, 2H, CH Ar), 6.47 (d, *J* 7.25 Hz, 1H, CH Ar), 6.95 (t, *J* 7.75 Hz, 1H, CH Ar), 7.25–7.38 (m, 4H, CH Ar) ppm; <sup>13</sup>C NMR (CDCl<sub>3</sub>):  $\delta$  21.56, 23.92, 27.82, 31.4, 42.0, 57.3, 110.5, 114.5, 118.7, 128.6, 129.0, 132.0, 138.9, 140.5, 147.0, 212.4 ppm. Anal. Calcd.

for  $\text{C}_{20}\text{H}_{22}\text{ClNO}$  (327.85): C, 73.27; H, 6.76; N, 4.27. Found: C, 73.01; H, 6.81; N, 4.39. MS (EI)  $m/z$  327 ( $\text{M}^+$ ).

2-[(4-Chloro-phenyl)-*p*-tolylamino-methyl]cyclohexanone (Table 2, entry 8): Yield: 88%, orange solid, *syn/anti*: 63/37, FT-IR:  $\nu_{\text{max}}$  (KBr): 3367 (NH stretch), 1697 (C=O stretch)  $\text{cm}^{-1}$ ;  $^1\text{H}$  NMR (250 MHz,  $\text{CDCl}_3$ ): 1.59–1.92 (m, 3H,  $\text{CH}_2$ ), 1.94–2.05 (m, 3H,  $\text{CH}_2$ ), 2.17 (s, 3H,  $\text{CH}_3$ ), 2.26 (m, 2H, CH), 2.81–2.85 (m, 1H, CH), 4.68 (d,  $J$  4.25 Hz, 0.63H, CH), 4.82 (d,  $J$  5.25 Hz, 0.37H, CH), 6.41 (d,  $J$  8.25 Hz, 2H, CH Ar), 6.89 (d,  $J$  8.25 Hz, 2H, CH Ar), 7.55 (d,  $J_1$  8.75 Hz,  $J_2$  4.75 Hz, CH Ar), 8.14 (d,  $J$  8.75 Hz, 2H, CH Ar) ppm. Anal. Calcd. for  $\text{C}_{20}\text{H}_{22}\text{ClNO}_2$ : C, 73.27; H, 6.76; N, 4.27. Found: C, 73.48; H, 6.43; N, 4.21.

2-((4-Chlorophenyl)(4-chlorophenylamino)methyl)cyclohexanone (Table 2, entry 9): Yield: 89%, white solid, *syn/anti*: 0/100, FT-IR:  $\nu_{\text{max}}$  (KBr): 3409.9 (NH stretch), 1701.1 (C=O stretch)  $\text{cm}^{-1}$ ;  $^1\text{H}$  NMR ( $\text{CDCl}_3$ ):  $\delta$  1.70–1.96 (m, 6H,  $\text{CH}_2$ ), 2.31–2.43 (m, 2H, CH), 2.73 (m, 1H, CH), 4.51 (d,  $J$  6.0 Hz, 1H, CH), 6.41 (d,  $J$  8.0 Hz, 2H, CH Ar), 7.0 (d,  $J$  7.75 Hz, 2H, CH Ar), 7.27–7.33 (m, 4H, CH Ar) ppm. Anal. Calcd. for  $\text{C}_{19}\text{H}_{19}\text{Cl}_2\text{ON}$ : C, 65.53; H, 5.50; N, 4.02. Found: C, 65.77; H, 5.64; N, 4.13.

2-((4-Chlorophenylamino)(4-nitrophenyl)methyl)cyclohexanone (Table 2, entry 11): Yield: 77%, white solid, *syn/anti*: 42/58, FT-IR:  $\nu_{\text{max}}$  (KBr): 3200 (NH stretch), 1654 (C=O stretch)  $\text{cm}^{-1}$ ;  $^1\text{H}$  NMR ( $\text{CDCl}_3$ ):  $\delta$  1.58–1.74 (m, 3H,  $\text{CH}_2$ ), 1.92–2.05 (m, 3H,  $\text{CH}_2$ ), 2.26–2.47 (m, 2H,  $\text{CH}_2$ ), 2.81–2.85 (m, 1H, CH), 4.62 (d,  $J$  4.75 Hz, 0.58H, CH), 4.79 (d,  $J$  3.5 Hz, 0.42H, CH), 6.41 (d,  $J$  8.75 Hz, 2H, CH Ar), 7.02 (d,  $J$  8.75 Hz, 2H, CH Ar), 7.53 (dd,  $J_1$  8.75 Hz,  $J_2$  3.5 Hz, 2H, CH Ar), 8.15 (d,  $J$  8.75 Hz, 2H, CH Ar) ppm. Anal. Calcd. for  $\text{C}_{19}\text{H}_{19}\text{ClN}_2\text{O}_3$ : C, 63.60; H, 5.34; N, 7.81. Found: C, 63.98; H, 5.84; N, 7.54.

2-[(4-Nitro-phenyl)-*m*-tolylamino-methyl]cyclohexanone (Table 2, entry 12): Yield: 80%, yellow solid, *syn/anti*: 37/63, FT-IR:  $\nu_{\text{max}}$  (KBr): 3367 (NH stretch), 1697 (C=O stretch)  $\text{cm}^{-1}$ ;  $^1\text{H}$  NMR ( $\text{CDCl}_3$ ): 1.59–1.92 (m, 3H,  $\text{CH}_2$ ), 1.94–2.05 (m, 3H,  $\text{CH}_2$ ), 2.17 (s, 3H,  $\text{CH}_3$ ), 2.26 (m, 2H, CH), 2.81–2.85 (m, 1H, CH), 4.68 (d,  $J$  5.25 Hz, 0.63H, CH), 4.82 (d,  $J$  4.25 Hz, 0.37H, CH), 6.41 (d,  $J$  8.25 Hz, 2H, CH Ar), 6.89 (d,  $J$  8.25 Hz, 2H, CH Ar), 7.55 (d,  $J_1$  8.75 Hz,  $J_2$  4.75 Hz, 2H,

CH Ar), 8.14 (d,  $J$  8.75 Hz, 2H, CH Ar) ppm. Anal. calcd. for  $\text{C}_{20}\text{H}_{22}\text{N}_2\text{O}_3$ : C, 70.99; H, 6.55; N, 8.28. Found: C, 71.34; H, 6.81; N, 8.59. MS (EI)  $m/z$  358 ( $\text{M}^+$ ).

2-[(4-Nitro-phenyl)-*p*-tolylamino-methyl]cyclohexanone (Table 2, entry 13): Yield: 75%, yellow solid, *syn/anti*: 36/64, FT-IR:  $\nu_{\text{max}}$  (KBr): 3382.9 (NH stretch), 1693.2 (C=O stretch)  $\text{cm}^{-1}$ ;  $^1\text{H}$  NMR ( $\text{CDCl}_3$ ):  $\delta$  1.57–1.75 (m, 3H,  $\text{CH}_2$ ), 1.85–2.06 (m, 3H,  $\text{CH}_2$ ), 2.19 (s, 3H), 2.31–2.41 (m, 2H, CH), 2.81–2.85 (m, 1H, CH), 4.69 (d,  $J$  5.0 Hz, 0.64H, CH), 4.84 (d,  $J$  4.25 Hz, 0.36H, 8-CH), 6.27 (d,  $J$  8.0 Hz, 2H, CH Ar), 6.49 (d,  $J$  6.5 Hz, 1H, CH Ar), 6.96 (t,  $J$  7.75 Hz, 1H, CH Ar), 7.53–7.58 (m, 2H, CH Ar), 8.15 (d,  $J$  8.75 Hz, 2H, CH Ar) ppm;  $^{13}\text{C}$  NMR ( $\text{CDCl}_3$ ):  $\delta$  21.5, 24.5, 25.0, 27.0, 27.7, 32.0, 42.4, 42.4, 56.2, 57.1, 57.2, 57.7, 110.4, 110.9, 114.4, 114.9, 119.1, 119.4, 123.7, 128.2, 128.6, 129.0, 129.1, 139.9, 146.6, 150.0, 160.4, 160.5, 211.1, 212.4 ppm. Anal. Calcd. for  $\text{C}_{20}\text{H}_{22}\text{N}_2\text{O}_3$ : C, 71.41; H, 5.98; N, 8.32. Found: C, 71.24; H, 5.87; N, 8.04.

2-((*m*-Toluidino)(4-hydroxyphenyl)methyl)cyclohexanone (Table 2, entry 14): Yield: 88%, orange solid, *syn/anti*: 0/100, FT-IR:  $\nu_{\text{max}}$  (KBr): 3200 (NH and OH stretch), 1660 (C=O stretch)  $\text{cm}^{-1}$ ;  $^1\text{H}$  NMR ( $\text{CDCl}_3$ ):  $\delta$  1.7–1.8 (m, 2H,  $\text{CH}_2$ ), 1.83–1.89 (m, 2H,  $\text{CH}_2$ ), 2.1–2.7 (m, 2H,  $\text{CH}_2$ ), 2.43 (s, 3H,  $\text{CH}_3$ ), 2.6 (t,  $J$  6.35 Hz, 2H, CH), 2.81–2.85 (m, 1H, CH), 4.29 (s, 1H, CH), 6.85–6.9 (m, 2H, CH Ar), 7.01–7.05 (m, 1H, CH Ar), 7.25–7.48 (m, 3H, CH Ar), 7.7 (d,  $J$  8.5 Hz, 2H, CH), 8.47 (s, OH) ppm. Anal. Calcd. for  $\text{C}_{20}\text{H}_{23}\text{NO}_2$ : C, 77.64; H, 7.48; N, 10.34. Found: C, 77.85; H, 7.62; N, 4.52. MS (EI)  $m/z$  309 ( $\text{M}^+$ ).

Additionally, reusability of the catalyst was investigated. After the completion of the reaction, the catalyst was sepa-

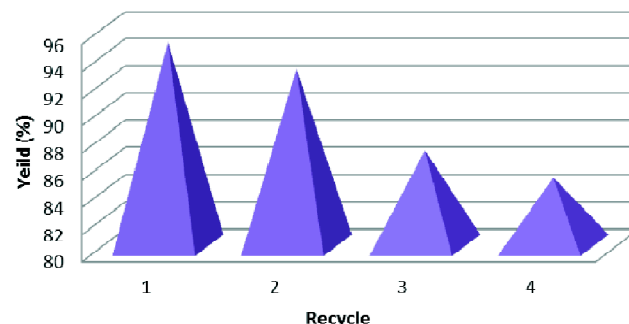


Fig. 5. The recyclability of the  $\text{Fe}_3\text{O}_4@\text{SiO}_2@\text{PrNH}_2\text{-Cu}$  MNPs in the synthesis of  $\beta$ -amino carbonyl compounds.

rated by using an external magnetic field. The recycled catalyst was washed with dichloromethane and subjected to a second reaction process. The results show that the yield of product after four runs was only slightly reduced (Fig. 5).

## Conclusion

We have developed a simple, clean, efficient and environmentally friendly approach for the one-pot synthesis of  $\beta$ -amino ketones by the three-component Mannich reaction of cyclohexanone, aromatic aldehydes, and anilines using  $\text{Fe}_3\text{O}_4@\text{SiO}_2@\text{PrNH}_2\text{-Cu}$  as a reusable nanocatalyst. The reaction proceeded smoothly and selectively in the presence of  $\text{Fe}_3\text{O}_4@\text{SiO}_2@\text{PrNH}_2\text{-Cu}$  and produced  $\beta$ -amino ketones in high yields and short reaction time at room temperature.

## Acknowledgements

We are thankful to the Research Council of Payame Noor University for the financial support of this study.

## References

1. V. Polshettiwar, R. Luque, A. Fihri, H. Zhu and M. Bouhrara, *Chem. Rev.*, 2011, **111**, 3036.
2. S. Laurent, D. Forge, M. Port, A. Roch, C. Robic, L. Vander Elst and R. N. Muller, *Chem. Rev.*, 2008, **108**, 2064.
3. M. Gawande, P. S. Branco and R. S. Varma, *Chem. Soc. Rev.*, 2013, **42**, 3371.
4. R. Hudson, Y. Feng, R. S. Varma and A. Moores, *Green Chem.*, 2014, **16**, 4493.
5. M. B. Gawande, Y. Monga, R. Zboril and R. K. Sharma, *Coord. Chem. Rev.*, 2015, **288**, 118.
6. Z. Zhang, J. Zhen, B. Liu, K. Lv and K. Deng, *Green Chem.*, 2015, **17**, 1308.
7. B. Karimi, F. Mansouri and H. M. Mirzaei, *Chem. Cat. Chem.*, 2015, **7**, 1736.
8. N. Jaffrezic-Renault, C. Martelet, Y. Chevolot and J.-P. Cloarec, *Sensors*, 2007, **7**, 589.
9. H. Gu, K. Xu, C. Xu and B. Xu, *Chem. Comm.*, 2006, 941.
10. J. Ying, R. M. Lee, P. S. Williams, J. C. Jeffrey, S. F. Sherif, B. Brian and Z. Maciej, *Biotechnol. Bioeng.*, 2007, **96**, 1139.
11. K. Müller, J. N. Skepper, N. Posfai, R. Trivedi, S. Howarth, C. Corot, E. Lancelot, P. W. Thompson, A. Brown and J. H. Gillard, *Biomaterials*, 2007, **28**, 1629.
12. Z. Liu and H. Mao, *J. Lumin.*, 2017, **190**, 179.
13. Y. Yao, S. Miao, S. Yu, L. P. Ma, H. Sun and S. Wang, *J. Colloid. Interf. Sci.*, 2012, **379**, 20.
14. M. F. Shao, F. Y. Ning, J. W. Zhao, M. Wei, D. G. Evans and X. Duan, *J. Am. Chem. Soc.*, 2012, **134**, 1071.
15. H. X. Che, S. J. Gwee, W. M. Ng, A. L. Ahmad and J. Lim, *Colloids Surf. A: Physicochem. Eng. Asp.*, 2018, **539**, 209.
16. Y. H. Deng, Y. Cai, Z. K. Sun, J. Liu, C. Liu, J. Wei, W. Li, Y. Wang and D. Y. Zhao, *J. Am. Chem. Soc.*, 2010, **132**, 8466.
17. B. V. S. Reddy, A. S. Krishna, A. V. Ganesh and G. G. K. S. N. Kumar, *Tetrahedron Lett.*, 2011, **52**, 1359.
18. B. Koo, H. Xiong, M. D. Slater, V. B. Prakapenka, M. Balasubramanian, P. Podsiadlo, C. S. Johnson, T. Rajh and E. V. Shevchenko, *Nano Lett.*, 2012, **12**, 2429.
19. Y. R. Chemla, H. L. Crossman, Y. Poon, R. McDermott, R. Stevens, M. D. Alper and J. Clarke, *Proc. Natl. Acad. Sci. USA*, 2000, **97**, 14268.
20. Y. Liu, Y. Gao and C. Xu, *Chin. Phys. B*, 2013, **22**, 097503.
21. Z. Lei, Y. Li and X. Wei, *J. Solid State Chem.*, 2008, **181**, 480.
22. Y. Deng, D. Qi, C. Deng, X. Zhang and D. Zhao, *J. Am. Chem. Soc.*, 2008, **130**, 28.
23. L. Sun, C. Zhang, L. Chen, J. Liu, H. Jin, H. Xu and L. Ding, *Anal. Chim. Acta*, 2009, **638**, 162.
24. Z. Zhang, L. Zhang, L. Chen, L. Chen and Q. H. Wan, *Biotechnol. Prog.*, 2006, **22**, 514.
25. K. Xu, C. Liu, K. Kang, Z. Zheng, S. Wang, Z. Tang and W. Yang, *Compos. Sci. Technol.*, 2018, **154**, 8.
26. P. Xie, Z. Wang, Z. Zhang, R. Fan, C. Cheng, H. Liu, Y. Liu, T. Li, C. Yan, N. Wang and Z. Guo, *J. Mater. Chem. C*, 2018, **6**, 5239.
27. Z. Wu, S. Gao, L. Chen, D. Jiang, Q. Shao, B. Zhang, Z. Zhai, C. Wang, M. Zhao, Y. Ma, X. Zhang, L. Weng, M. Zhang and Z. Guo, *Macromol. Chem. Phys.*, 2017, **218**, 1700357.
28. T. Tamoradi, A. Ghorbani-Choghmarani and M. Ghadermazi, *Polyhedron*, 2018, **145**, 120.
29. M. Darabi, T. Tamoradi, M. Ghadermazi and A. Ghorbani-Choghmarani, *Transition Met. Chem.*, 2017, **42**, 703.
30. E. F. Vansant, P. Van Der Voot and K. C. Vrancken, *Stud. Surf. Sci. Catal.*, 1995, **93**, 193.
31. M. Arend, B. Westermann and N. Risch, *Angew. Chem. Int. Ed.*, 1998, **37**, 1044.
32. S. Kobayashi and H. Ishitani, *Chem. Rev.*, 1999, **99**, 1069.
33. S. Kobayashi and M. Ueno, "Comprehensive Asymmetric Catalysis", Springer, Berlin, 2004.
34. R. Duthaler, *Angew. Int. Ed. Engl.*, 2003, **42**, 975.
35. K. Manabe, Y. Mori and S. Kobayashi, *Tetrahedron*, 2001, **57**, 2537.
36. Y. Dai, B. D. Li, H. D. Quan and C. X. Lu, *Chin. Chem. Lett.*, 2010, **21**, 31.
37. M. Z. Kassaei, R. Mohammadi, H. Masrouri and F.

Hassani *et al.*: Synthesis, characterization and application of  $\text{Fe}_3\text{O}_4@\text{SiO}_2@\text{PrNH}_2\text{-Cu}$  as a novel and highly efficient *etc.*

- Movahedi, *Chin. Chem. Lett.*, 2011, **22**, 1203.
38. M. Terada, K. Sorimachi and D. Uraguchi, *Synlett.*, 2006, 133.
39. A. A. Jafari and F. Moradgholi, *Acta Chim. Slov.*, 2009, **56**, 744.
40. (a) M. A. Nasser, B. Zakerinasab and M. Samieadel, *RSC Adv.*, 2014, **79**, 41753; (b) B. Zakerinasab, M. A. Nasser, H. Hassani and M. Samieadel, *Res. Chem. Intermed.*, 2016, **42**, 3169; (c) R. C. Martins, N. Amaral-Silva and R. M. Quinta-Ferreira, *Appl. Catal. B*, 2010, **99**, 135.
41. H. Hassani, B. Zakerinasab, M. A. Nasser and M. Shavakandi, *RSC Adv.*, 2016, **6**, 17560.
42. J. Sun, G. Yu, L. Liu, Z. Li, Q. Kan, Q. Huo and J. Guan, *Catal. Sci. Technol.*, 2014, **4**, 1246.
43. A. Hasanpour, M. Niyafar and M. H. J. Amighian, *J. Phys. Chem. Solids*, 2012, **73**, 1066.
44. N. Azizi, L. Torkiyan and M. R. Saidi, *Org. Lett.*, 2006, **8**, 2079.
45. A. R. Massah, R. J. Kalbasi and N. Samah, *Bull. Korean Chem. Soc.*, 2011, **32**, 1703.
46. W.-B. Yi, C. Cai, *J. Fluorine Chem.*, 2006, **127**, 1515.
47. W. Shen, L.-M. Wang and H. Tian, *J. Fluorine Chem.*, 2008, **129**, 267.
48. Y. Y. Yang, W. G. Shou and Y. G. Wang, *Tetrahedron*, 2006, **62**, 10079.
49. H. Eshghi, M. Rahimizadeh, M. Hosseini and A. Javadian-Saraf, *Monatsh. Chem.*, 2013, **144**, 197.
50. M. A. Bigdeli, F. Nemati and G. H. Mahdavinia, *Tetrahedron Lett.*, 2007, **48**, 6801.
51. K. Gong, D. Fang, H. Wang and Z. Liu, *Monatsh. Chem.*, 2007, **138**, 1195.
52. F. Nemati, A. S. Fakhaei, A. Amoozadeh and Y. Saeidi Hayeniaz, *Synth. Commun.*, 2011, **41**, 3695.
53. F. Moradgholi, J. Lari, M. Vahidi Parsa and M. Mirkharrazi, *Acta Chim. Slov.*, 2016, **63**, 781.

